PHILOSOPHICAL TRANSACTIONS A

rsta.royalsocietypublishing.org

Research

Article submitted to journal

Subject Areas:
Applied Mathematics, Fluid Mechanics

Keywords:
solitary waves, interfacial, hydroelastic

Author for correspondence:
Emilian I. Părău
e-mail: e.parau@uea.ac.uk

THE ROYAL SOCIETY PUBLISHING

Solitary interfacial hydroelastic waves

Emilian I. Părău[1]

[1]School of Mathematics, University of East Anglia, Norwich, NR4 7TJ, UK

Solitary waves travelling along an elastic plate present between two fluids with different densities are computed in this paper. Different two-dimensional configurations are considered: the upper fluid can be of infinite extent, bounded by a rigid wall or under a second elastic plate. The dispersion relation is obtained for each case and numerical codes based on integro-differential formulations for the full nonlinear problem are derived.

1. Introduction

There is a growing interest in recent years in the study of hydroelasticity, where an elastic plate is interacting with a fluid [1]. This is motivated by the large number of applications, such as the study of waves under ice plates in polar regions [2] where the ice plate can be modelled as an elastic plate.

Solitary hydroelastic waves have been studied extensively in a number of papers [3–9], where branches of solutions and the evolution in time was discussed. In most papers investigating nonlinear hydroelastic waves, the fluid is assumed to be under the elastic plate. However, there are other physical problems where an elastic plate separates two fluids. One example is in flat-plate-type fuel assemblies used in the cooling systems of nuclear reactors [10], where there are layers of fluids separated by parallel elastic plates. Another example is the flapping of an elastic flap in an axial flow, which have a number of medical applications [11]. There are also icy moons of Jupiter and Saturm where layered oceans separated by ice plates are hypothesized to exist (e.g. on Ganymede).

Very recently, the well-posedness of interfacial hydroelastic waves have been studied [12,13], where the elastic plate is placed between two fluids of different densities. The authors have used a vortex sheet formulation and both cases of a heavy and a massless elastic plate were considered.

© The Authors. Published by the Royal Society under the terms of the Creative Commons Attribution License http://creativecommons.org/licenses/by/4.0/, which permits unrestricted use, provided the original author and source are credited.

Results on the existence of periodic travelling interfacial hydroelastic waves in infinite depth [14] have been obtained by proving a global bifurcation theorem and some numerical computations of periodic waves were also presented.

In a related problem, nonlinear travelling waves on a sheet of fluid bounded by elastic plates have been computed in the absence of gravity [15]. One-dimensional time-dependent equations were also derived based on a long-wavelength approximation in this configuration and the temporal evolution of disturbances is investigated numerically [16].

When there is more than one interface (or elastic plate), the problem is more complicated to analyse due to interaction between different modes. Computations of solitary gravity and gravity-capillary waves for full Euler equations in two-layer configurations in the presence of a free surface have been performed recently [17–20] and different type of solutions have been found, where the interface and free surface are in phase or out of phase, depending on their velocity. Wang *et al.* [21] have computed solitary waves and generalised solitary waves for a stratified fluid under an elastic plate, which models the structure of water in frozen lakes in polar regions.

In this paper we will consider a massless elastic plate between two fluids of different densities in two-dimensions, with the heavier fluid lying below. The fluids are assumed to be incompressible, inviscid and the flow irrotational in each layer. The elastic plate will be modelled using the special Cosserat theory of hyperelastic shells, satisfying Kirchhoff hypothesis [22]. The lighter fluid on top is either bounded by a rigid wall, or by another elastic plate. The numerical method employed to calculate interfacial gravity-capillary solitary waves [19,23] is generalised to compute hydroelastic interfacial waves. In the next section the formulation of the problem is presented. The dispersion relation is analysed, followed by the description of the numerical method. Some computational results are presented in section 5 and a discussion concludes the paper.

2. Formulation

We consider two superposed fluids separated by an elastic plate in two dimensions. The heavier fluid with constant density ρ_1 lies below the elastic plate, while the lighter fluid has constant density ρ_2 and lies on top of the elastic plate. Both fluids are assumed inviscid, incompressible and the flow is irrotational in each layer. The elastic plate of flexural rigidity D_1 is assumed to be thin and is modelled according to the special Cosserat theory of hyperelastic shells [22]. At rest, the lower fluid upper fluid has a constant depth h_1^* and the upper fluid a depth h_2^* and they are bounded by rigid walls. However, we will also consider cases when one or both fluids are of infinite depth (see Figure 1, left), or when the upper rigid wall is replaced by a second elastic plate with a flexural rigidity D_2 (see Figure 1, right).

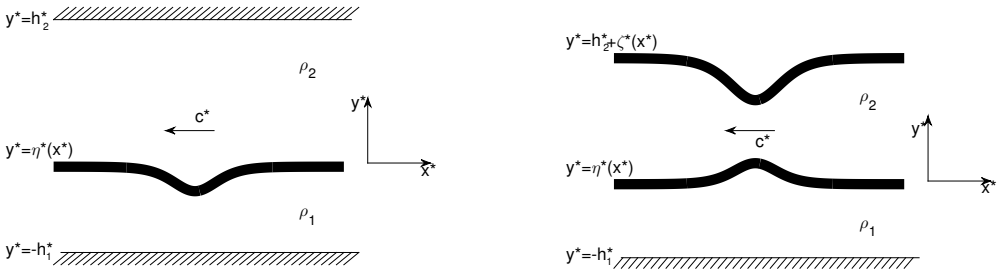

Figure 1. Sketch of the problem. Al the physycal dimensional variables are denoted with starred letters. Left: the fluids are bounded below and above by rigid walls. Right: the upper wall is replaced by a second elastic plate.

We will non-dimensionalize the physical variables by using the following length and velocity scales [4–6]

$$l=\left(\frac{D_1}{\rho_1 g}\right)^{1/4}, \qquad v=\left(\frac{D_1 g^3}{\rho_1}\right)^{1/8}.$$

The following non-dimensional parameters are introduced

$$h_1=\frac{h_1^*}{l}, \quad h_2=\frac{h_2^*}{l}, \quad R=\frac{\rho_2}{\rho_1}, \quad D=\frac{D_2}{D_1}.$$

Cartesian coordinates x and y are introduced with the x-axis along the undisturbed elastic plate and the vertical upward y-axis. We are interested in steady waves which propagates with (non-dimensional) constant velocity c in the horizontal direction and we choose a frame of reference moving with this speed. In this frame of reference, the equations of motion for the velocity potentials in lower and upper fluids $\Phi_1(x,y)$, $\Phi_2(x,y)$ and for the elastic plate $y=\eta(x)$ are given by

$$\nabla^2\Phi_1=0, \qquad \text{for } -h_1<y<\eta(x), \tag{2.1}$$

$$\nabla^2\Phi_2=0, \qquad \text{for } \eta(x)<y<h_2, \tag{2.2}$$

with the kinematic and dynamic conditions on the elastic plate

$$\Phi_{1_x}\eta_x=\Phi_{1_y}, \qquad \Phi_{2_x}\eta_x=\Phi_{2_y}, \qquad \text{for } y=\eta(x), \tag{2.3}$$

$$\begin{aligned}&\frac{1}{2}\left(|\nabla\Phi_1|^2-R|\nabla\Phi_2|^2\right)+(1-R)\eta+\frac{1}{2}\left(\frac{\eta_{xx}}{(1+\eta_x^2)^{3/2}}\right)^3\\&+\frac{1}{\sqrt{1+\eta_x^2}}\partial_x\left[\frac{1}{\sqrt{1+\eta_x^2}}\partial_x\left(\frac{\eta_{xx}}{(1+\eta_x^2)^{3/2}}\right)\right]=\frac{c^2}{2}(1-R), \qquad \text{for } y=\eta(x),\end{aligned} \tag{2.4}$$

and no-flow conditions on the bed and on the upper wall

$$\Phi_{1_y}=0 \qquad \text{for } y=-h_1, \qquad \text{and} \qquad \Phi_{2_y}=0 \qquad \text{for } y=h_2. \tag{2.5}$$

If one or both of the fluids are of infinite extent, the no-flow conditions on the bed and on the upper wall (2.5) are replaced by

$$\nabla\Phi_1\to 0, \qquad \text{as } y\to-\infty, \qquad \text{and/or} \qquad \nabla\Phi_2\to 0 \qquad \text{as } y\to\infty. \tag{2.6}$$

When the upper wall is replaced by the second elastic plate the no-flow condition at $y=h_2$ is substituted by a kinematic and a dynamic condition at the new elastic plate at $y=h_2+\zeta(x)$

$$\Phi_{2_x}\zeta_x=\Phi_{2_y}, \qquad \text{for } y=h_2+\zeta(x) \tag{2.7}$$

$$\frac{1}{2}|\nabla\Phi_2|^2+\zeta+\frac{D}{R}\left\{\frac{1}{2}\left(\frac{\zeta_{xx}}{(1+\zeta_x^2)^{3/2}}\right)^3+\frac{1}{\sqrt{1+\zeta_x^2}}\partial_x\left[\frac{1}{\sqrt{1+\zeta_x^2}}\partial_x\left(\frac{\zeta_{xx}}{(1+\zeta_x^2)^{3/2}}\right)\right]\right\}=\frac{c^2}{2}. \tag{2.8}$$

We have assumed that the elastic plate(s) to be not pre-stressed and we neglect the stretching of the plate(s). The inertia of the thin elastic plate(s) is neglected, so the plate(s) acceleration term is not considered here.

3. Dispersion relation

By considering small perturbations of the form e^{ikx} of the rest state, we can, after some algebra, derive the dispersion relation between the phase speed and k. In the case of one elastic plate we

obtain

$$c_i^2(k) = \frac{1}{k}\frac{(1-R+k^4)\tanh(kh_1)\tanh(kh_2)}{R\tanh(kh_1)+\tanh(kh_2)}. \tag{3.1}$$

We consider here only the physical configuration when $0 \le R < 1$, $h_1 > 0$ and $h_2 > 0$. It can easily be observed that

$$c_i \to c_{i_0} = \sqrt{\frac{(1-R)h_1h_2}{Rh_1+h_2}} \quad \text{as } k \to 0.$$

If either of the fluid is of infinite c_i approaches infinity as k approaches zero. Also, by considering for example the Taylor series of $c_i(k)$ at $k = 0$,

$$c_i(k) = c_{i_0} - \frac{c_{i_0}}{6}\frac{h_1h_2(Rh_2+h_1)}{Rh_1+h_2}k^2 + O(k^4),$$

it can be observed that $c_i(k)$ is decreasing for $k > 0$, (k small) and then increases to infinity as $k \to \infty$. This show there is always a minimum value of $c_i(k)$, which we denote by $c_{i_{min}}$ at a finite value of $k = k_{min} > 0$. When either of fluids is of infinite extent, c_{i_0} becomes infinite. If both fluids are of infinite extent an explicit value for c_{min} is found:

$$c_{i_{min}} = \frac{2}{3^{3/8}} \cdot \frac{(1-R)^{3/8}}{(1+R)^{1/2}}.$$

It is worth noting that if $R = 0$ we recover the value of c_{min} of one fluid under an elastic plate [4].

When the upper wall is replaced by the second elastic plate, the dispersion relation is more complex and becomes

$$c_\pm^2(k) = \frac{b(k) \pm \sqrt{b^2(k) - 4a(k)d(k)}}{2ka(k)}, \tag{3.2}$$

where $c_+(k)$ correspond to the 'fast' mode and $c_-(k)$ to the 'slow' mode, and

$$a(k) = 1 + R\tanh(kh_1)\tanh(kh_2),$$

$$b(k) = \tanh(kh_1) + \tanh(kh_2) + k^4\left[\tanh(kh_1) + \frac{D}{R}(R\tanh(kh_1) + \tanh(kh_2))\right],$$

$$d(k) = \tanh(kh_1)\tanh(kh_2)(k^4 + 1 - R)\left(\frac{D}{R}k^4 + 1\right).$$

It can be easily seen that

$$c_\pm \to c_{\pm_0} = \frac{h_1 + h_2 \pm \sqrt{h_1^2 + h_2^2 - 2h_1h_2 + 4h_1h_2R}}{2}, \quad \text{as } k \to 0,$$

and that $c_\pm$ increases to infinity as $k \to \infty$. As before, by expanding in Taylor series around $k = 0$, it can be shown that both $c_+(k)$ and $c_-(k)$ have a minimum for any value of the parameters, which is different for the gravity-capillary case where the existence of the minimum depends on the surface tension [19]. The functions c_i, when an upper wall is present, and $c_\pm$, when the wall is replaced with an elastic plate, are plotted in Figure 2 for some values of parameters. It can be observed that c_i is following closely c_- and the minima of c_i and c_- are very close to the long-wave limits c_{i_0} and c_{-_0} for these values of parameters ($h_1 = h_2 = 1$ and $R = 0.9$, $D = 1$). When only one finite-depth fluid was considered, Guyenne and Părău [5] have derived a 5th order KdV equation valid near the long-wave limit phase speed. By varying the parameters, the qualitative picture does not change, unless both fluid become infinite (see Figure 2, right).

As we are interested in solitary waves, we will concentrate on regions of the spectrum where c is lower than the minimum of either c_i in the rigid lid case, or below the minimum of c_- in the two elastic plates case.

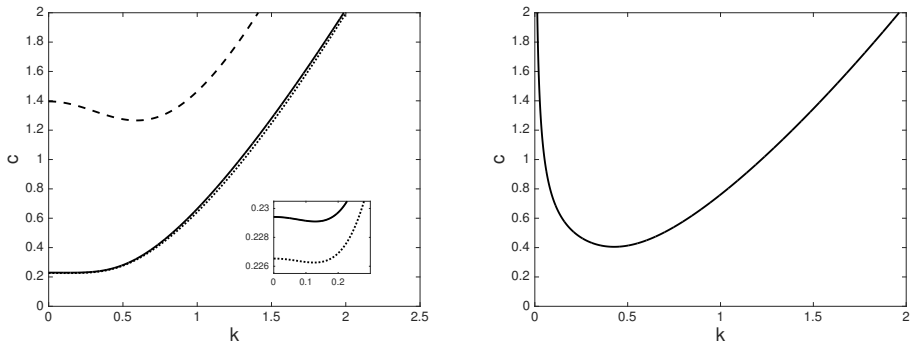

Figure 2. Left: the dispersion relation for $h_1 = h_2 = 1$ and $R = 0.9$, $D = 1$. The function c_i in the case of an upper wall is plotted with solid line. For the two elastic plates case c_+ is plotted with dashed line and c_- with dotted line. In the inset a close-up near the minimum values of c_i and c_- is shown. Right: the dispersion relation showing c_i in the infinite depth case ($h_1 = h_2 = \infty$, $R = 0.9$).

4. Numerical methods

To compute symmetric solitary waves, we will extend two numerical methods based on boundary integral equations techniques developed for gravity-capillary waves by Laget and Dias [23] and, respectively, Woolfenden and Părău [19], by replacing the surface tension with flexural effects [4,5]. We will recall here only the main ideas of these methods and refer the reader to these two papers for details.

In both cases complex potentials $w_j = \Phi_j + \mathrm{i}\Psi_\mathrm{j}$ are introduced in each fluid, $j = 1, 2$, where Ψ_j are the streamfunctions. The physical plane $z = x(w_j) + \mathrm{i}y(w_j)$ is mapped into the inverse plane w_j in each layer. We can set $\Psi_1 = \Psi_2 = 0$ on the thin elastic plate without loosing generality. In terms of the velocity potentials, the elastic plate profile is denoted

$$(x(\Phi_1), y(\Phi_1)) = (x(\Phi_1 + \mathrm{i}\,0), y(\Phi_1 + \mathrm{i}\,0)) = (x(\Phi_2 + \mathrm{i}\,0), y(\Phi_2 + \mathrm{i}\,0)),$$

and the link between the potentials is $\Phi_2 = g(\Phi_1)$, where g is unknown (see also [24] for more details).

Now, in the first case, when there is only one elastic plate, it can be shown that $\Psi_1 = -ch_1$ on the bed and $\Psi_2 = ch_2$ on the upper wall. By applying Cauchy formula in each layer and using the reflection in the rigid walls, it can be shown

$$\begin{aligned} x'(\Phi_0) - \frac{1}{c} = &-\frac{1}{\pi}\int_0^\infty y'(\Phi_1)\left(\frac{1}{\Phi_1 - \Phi_0} + \frac{1}{\Phi_1 + \Phi_0}\right)\mathrm{d}\Phi_1 \\ &+\frac{1}{\pi}\int_0^\infty \frac{(\Phi_0 - \Phi_1)y'(\Phi_1) + 2ch_1(x'(\Phi_1) - 1/c)}{(\Phi_1 - \Phi_0)^2 + 4c^2h_1^2}\mathrm{d}\Phi_1 \\ &+\frac{1}{\pi}\int_0^\infty \frac{-(\Phi_0 + \Phi_1)y'(\Phi_1) + 2ch_1(x'(\Phi_1) - 1/c)}{(\Phi_1 + \Phi_0)^2 + 4c^2h_1^2}\mathrm{d}\Phi_1, \end{aligned} \tag{4.1}$$

and

$$\begin{aligned} \frac{x'(\Phi_0)}{g'(\Phi_0)} - \frac{1}{c} = &\frac{1}{\pi}\int_0^\infty y'(\Phi_1)\left(\frac{1}{g(\Phi_1) - g(\Phi_0)} + \frac{1}{g(\Phi_1) + g(\Phi_0)}\right)\mathrm{d}\Phi_1 \\ &+\frac{1}{\pi}\int_0^\infty \frac{(g(\Phi_1) - g(\Phi_0))y'(\Phi_1) + 2ch_2(x'(\Phi_1) - g'(\Phi_1)/c)}{(g(\Phi_1) - g(\Phi_0))^2 + 4c^2h_2^2}\mathrm{d}\Phi_1 \\ &+\frac{1}{\pi}\int_0^\infty \frac{(g(\Phi_1) + g(\Phi_0))y'(\Phi_1) + 2ch_2(x'(\Phi_1) - g'(\Phi_1)/c)}{(g(\Phi_1) + g(\Phi_0))^2 + 4c^2h_2^2}\mathrm{d}\Phi_1. \end{aligned} \tag{4.2}$$

In these equations, Φ_0 is on the elastic plate, the primes denote differentiation with respect to Φ_1. and the first integral in each of the right-hand side of the equations (4.1) and (4.2) is evaluated in

the principal value sense. If h_1 and/or h_2 are infinite, the second and the third integrals vanish in the equations (4.1) and/or (4.2). The Bernoulli equation on the elastic plate becomes in the new variables

$$\frac{1}{2}\left(\frac{1-Rg'^2}{x'^2+y'^2}-c^2(1-R)\right)+(1-R)y+\frac{1}{2}\left(\frac{y''x'-y'x''}{x'^2+y'^2)^{3/2}}\right)^3+\frac{S}{(x'^2+y'^2)^{9/2}}=0, \tag{4.3}$$

where

$$\begin{aligned} S &= x'^5y^{(iv)}+2x'^3y'^2y^{(iv)}+x'y'^4y^{(iv)}-6x'^4x''y'''-2x'^2y'^2x''y''' \\ &+4x''y'^4y'''-x'^4x^{(iv)}y'-2x'^2x^{(iv)}y'^3-x^{(iv)}y'^5-4x'^4x'''y'' \\ &+2x'^2x'''y'^2y''+6x'''y'^4y''-10x'^3y'y''y'''+10x'^3x''x'''y' \\ &+10x'x''x'''y'^3-10x'y'^3y''y'''-39x'x''^2y'^2y''+3x''^3y'^3-3x'^3y''^3 \\ &+15x'y'^2y''^3+39x'^2x''y'y''^2-15x''y'^3y''^2+15x'^3x''^2y''-15x'^2x''^3y'. \end{aligned}$$

The equations (4.1)-(4.3) are solved for the unknowns x', y' and g' by discretising the potential Φ_1 on n points and solving the resulting nonlinear system by Newton's method. To obtain solitary waves, forced solutions are calculated initially for $c<c_{i_{min}}$ using an artificial pressure on the elastic plate and then, by removing the pressure, pure solitary waves are found for different values of parameters h_1, h_2 and R.

In the second case, when the upper wall is replaced by a second elastic plate, the equation (4.2) is replaced by two other equations obtained by applying Cauchy formula for evaluation points on the lower elastic plate and the upper one. If the upper elastic plate profile is denoted

$$(X(\Phi_1),Y(\Phi_1))=(x(\Phi_2+\mathrm{i}\,ch_2),y(\Phi_2+\mathrm{i}\,ch_2)),$$

the two equations are

$$\begin{aligned} \frac{x'(\Phi_0)}{g'(\Phi_0)}-\frac{1}{c} &= -\frac{1}{\pi}\int_0^\infty y'(\Phi_1)\left(\frac{1}{g(\Phi_1)-g(\Phi_0)}+\frac{1}{g(\Phi_1)+g(\Phi_0)}\right)\mathrm{d}\Phi_1 \\ &+\frac{1}{\pi}\int_0^\infty \frac{ch_2(X'(\Phi_1)-g'(\Phi_1)/c)-(g(\Phi_1)-g(\Phi_0))Y'(\Phi_1)}{(g(\Phi_1)-g(\Phi_0))^2+c^2h_2^2}\mathrm{d}\Phi_1 \\ &+\frac{1}{\pi}\int_0^\infty \frac{ch_2(X'(\Phi_1)-g'(\Phi_1)/c)-(g(\Phi_1)+g(\Phi_0))Y'(\Phi_1)}{(g(\Phi_1)+g(\Phi_0))^2+c^2h_2^2}\mathrm{d}\Phi_1, \end{aligned} \tag{4.4}$$

and

$$\begin{aligned} \frac{X'(\Phi_0)}{g'(\Phi_0)}-\frac{1}{c} &= -\frac{1}{\pi}\int_0^\infty Y'(\Phi_1)\left(\frac{1}{g(\Phi_1)-g(\Phi_0)}+\frac{1}{g(\Phi_1)+g(\Phi_0)}\right)\mathrm{d}\Phi_1 \\ &+\frac{1}{\pi}\int_0^\infty \frac{ch_2(x'(\Phi_1)-g'(\Phi_1)/c)+(g(\Phi_1)-g(\Phi_0))y'(\Phi_1)}{(g(\Phi_1)-g(\Phi_0))^2+c^2h_2^2}\mathrm{d}\Phi_1 \\ &+\frac{1}{\pi}\int_0^\infty \frac{ch_2(x'(\Phi_1)-g'(\Phi_1)/c)+(g(\Phi_1)+g(\Phi_0))y'(\Phi_1)}{(g(\Phi_1)+g(\Phi_0))^2+c^2h_2^2}\mathrm{d}\Phi_1. \end{aligned} \tag{4.5}$$

The first integral in each of the right-hand side of the equations (4.4) and (4.5) is evaluated in the principal value sense.

The Bernoulli equation on the upper elastic plate becomes

$$\frac{1}{2}\left(\frac{g'^2}{X'^2+Y'^2}-c^2\right)+Y+\frac{1}{2}\left(\frac{Y''X'-Y'X''}{X'^2+Y'^2)^{3/2}}\right)^3+\frac{\tilde{S}}{(X'^2+Y'^2)^{9/2}}=0, \tag{4.6}$$

where $\tilde{S}$ is similar with the one from the Bernoulli equation at the interfacial elastic plate, but with the variables X and Y instead of x and y. The system (4.1), (4.6)-(4.5) is then solved for x', y', g', X', Y' following the method described in detail by Woolfenden and Părău [19].

Most results in the case of an upper wall presented here are obtained with $n=800$ and $\Delta\Phi_1=0.05$, and the accuracy was checked varying the grid spacing. When the upper wall is replaced by an elastic plate typically $n=601$ were used and $\Delta\Phi_1=0.066$.

5. Results

(a) One elastic plate

We consider first the case of two fluids of infinite extent, $h_1 = h_2 = \infty$ and $R = 0.9$. Depression and elevation solitary waves have been computed for $c < c_{i_{min}} \approx 0.4053$ (see Figure 3). They have decaying oscillations in the direction of propagation and they start at a finite amplitude at $c = c_{i_{min}}$, not from zero. The branch of elevation has a more complicated behaviour and we show it here only partially, due to numerical difficulties in following it (see Wang *et al.* [25] for the one fluid $R = 0$ case) . When c decreases the wave start to overturn (see Figure 3, top right). A similar behaviour was observed in the one fluid ($R = 0$) problem under an elastic plate by Guyenne and Părău [4]. They have derived a defocusing nonlinear Schrödinger equation which cannot have as solutions small-amplitude solitons (see also [25], [6]).

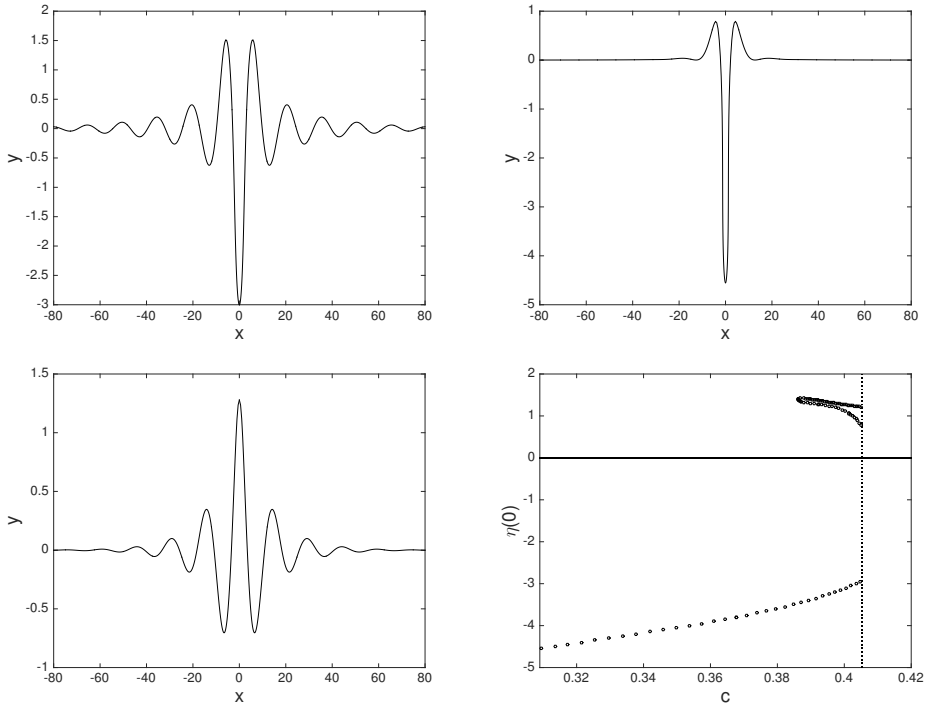

Figure 3. Examples of solitary waves for $h_1 = h_2 = \infty$ and $R = 0.9$. Top: depression solitary waves $c = 0.403$ (left), $c = 0.31$ (right). Bottom left: elevation solitary wave $c = 0.392$. Bottom right: amplitudes of branches of solitary waves shown with circles. The value of $c_{i_{min}}$ =0.4053 is shown with dotted line

We will consider next the case where both fluids are of finite depth, $h_1 = h_2 = 1$ and $R = 0.9$. Depression and elevation solitary waves have been obtained and there are some differences compared with the infinite depth case (see Figure 4). The branches of solitary waves seem to start from zero-amplitude at $c = c_{i_{min}} = 0.229$, not from a finite amplitude. They are characterised by a big pulse and much smaller oscillations on each side than in the infinite depth case. As the speed was approaching zero, we did not observe solutions with overturning profiles of solutions, as in the infinite depth case. However, we cannot follow the branch down to $c = 0$ because our solutions need to satisfy $x'(\Phi_1) \to 1/c$ as $\phi_1 \to \infty$. The elevation branch has again a more complicated shape than the depression one, with at least a turning point.

It is worth reminding here that the NLS equation which was derived for the one fluid case $R = 0$ becomes focusing if the depth is small, hence admitting small-amplitude solitons (see Wang *et al.* [25], Guyenne and Părău [5]), so we expect that a similar type of NLS can be derived in the interfacial case.

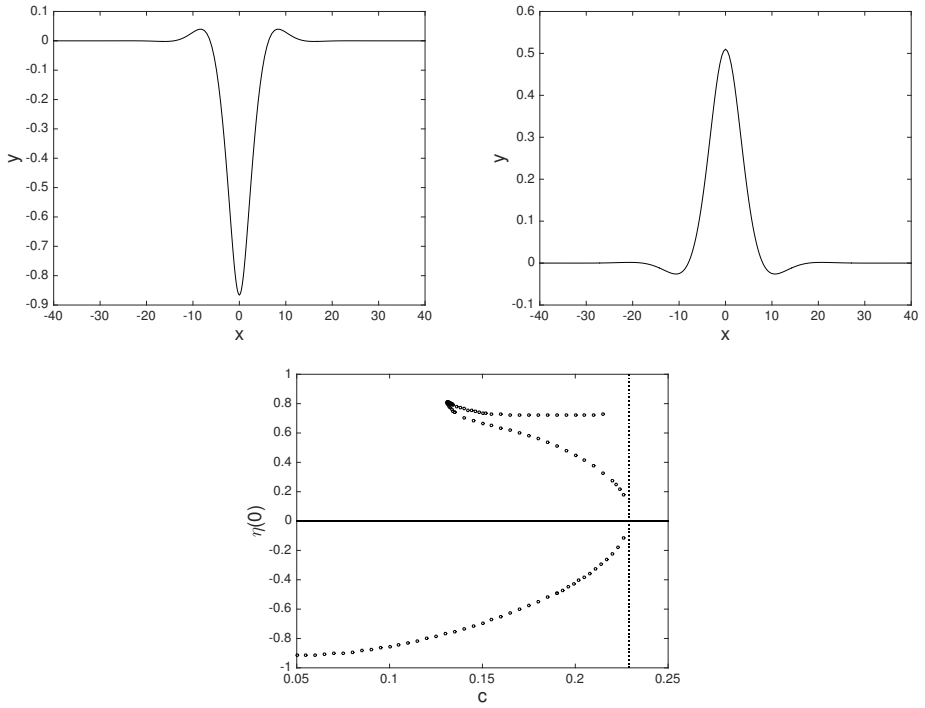

Figure 4. Examples of solitary waves for $h_1 = h_2 = 1$ and $R = 0.9$. Top left: depression solitary waves $c = 0.095$ (left) Top right: elevation solitary wave $c = 0.19$. Bottom: amplitudes of branches of solitary waves shown with circles. The value of $c_{i_{min}}$ =0.229 is shown with dotted line

(b) Two elastic plates

If we replace the upper wall with another elastic plate, we expect to find solitary waves only below the minimum of $c_-(k)$ as between the two branches $c_-(k)$ and $c_+(k)$ of the dispersion relation there is no gap in the spectrum (both $c_\pm(k) \to \infty$ as $k \to \infty$).

We consider the case $h_1 = \infty$, $h_2 = 1$ and $R = 0.9$, $D = 1$ as an example and Figure 5 shows a typical solitary wave solution. There is an elevation wave on the interfacial elastic plate and a depression solitary wave on the upper elastic plate, being out-of-phase. The main pulses are followed by smaller oscillations which are growing when approaching c_{-min} . The solitary waves branch bifurcates from $c_{-min} = 0.29$ at zero-amplitude, but is difficult to follow numerically the branch up to that point.

Another type of out-of-phase waves were also found, which are of depression type on the interfacial elastic plate and of elevation on the upper elastic plate (see Figure 6). It can be observed that these solutions have a depression wave of a smaller amplitude on the interfacial elastic plates than the two much bigger elevations neighbouring it and the situation is the opposite on the upper elastic plate.

It is worth mentioning that as we are interested only on steady waves in this paper, we have considered just waves travelling wth the same speed c along both elastic plates. However, in a

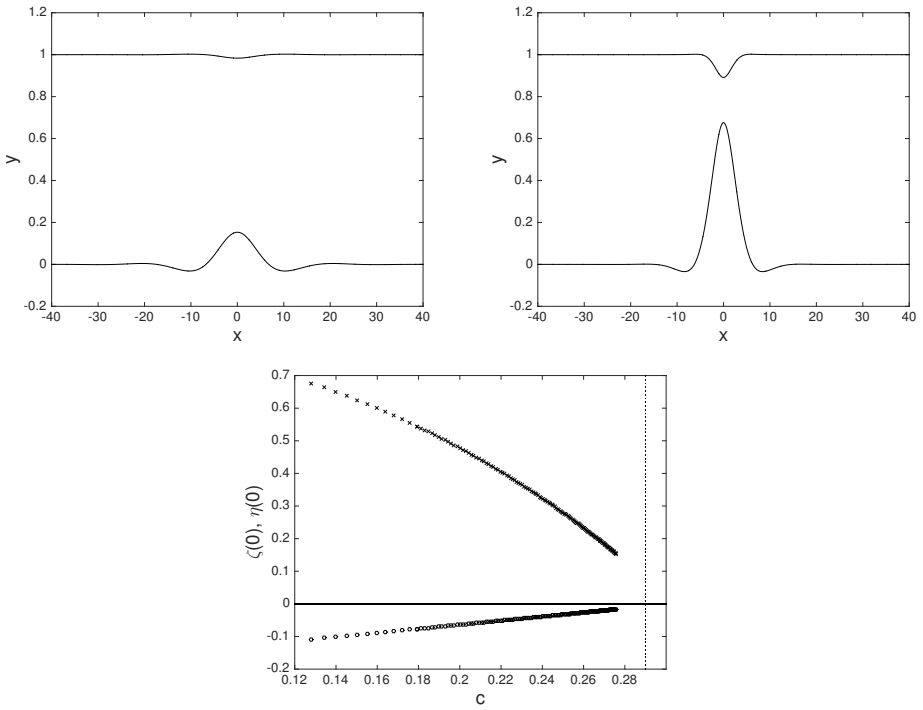

Figure 5. Examples of elevation solitary waves for $h_1 = \infty$, $h_2 = 1$ and $R = 0.9$, $D = 1$. Top: solitary waves $c = 0.276$ (left) and $c = 0.128$ (right). Bottom: amplitudes of branches of solitary waves shown with circles on free surface and with crosses on the interface. The value of c_{-min} =0.29 is shown with dotted line

related problem, Craig *et al.* [26] highlighted the physical relevance of resonance between internal and surface waves in a two-layer ocean when the speeds are different, and a similar study may be performed in the present configuration.

6. Conclusion

We have presented in this paper numerical results by calculating symmetric interfacial solitary waves when an elastic plate is separating two fluids of different densities. The gravity and the flexural effect have been included. After analysing the dispersion relation, depression and elevation solitary waves have been computed for fluids of infinite extent or of finite depth. Due to the large number of parameters we have restricted ourselves to a couple of cases only, but intensive numerical tests have shown results to be qualitatively similar with the ones presented here.

When the upper wall is replaced by a second elastic plate the solitary waves at the interfacial elastic plate and the upper one are out-of-phase and they bifurcate from the 'slow' mode. Gravity-capillary interfacial solitary waves in a similar setting, without elastic plates, but considering the effect of surface tension on both the free surface and interface have been computed before by Woolfenden and Părău [19]. One significant difference is that in the problem considered here there is always a minimum of the 'slow' mode, so we always expect an oscillatory decay of the solitary waves and not a monotonic one as in some cases in Woolfenden and Părău [19].

The numerical algorithms developed to calculate the solitary waves generalise the methods described by Laget and Dias [23] and by Woolfenden and Părău [19] by including flexural effects and are based on boundary integral equation methods, Cauchy formula, parameter continuation and Newton method.

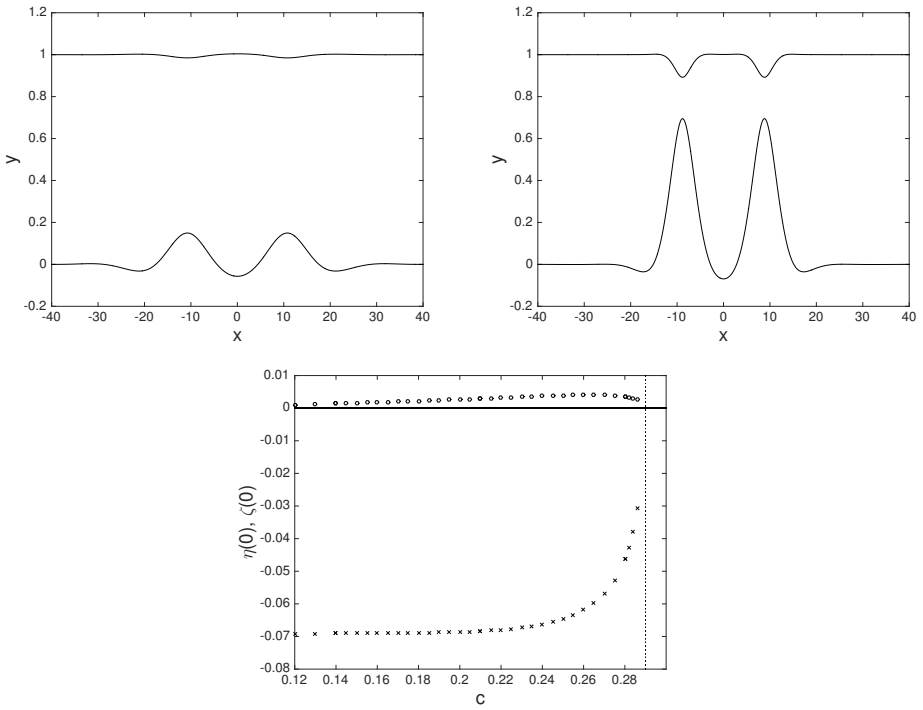

Figure 6. Examples of depression interfacial solitary waves for $h_1 = \infty$, $h_2 = 1$ and $R = 0.9$, $D = 1$. Top: solitary waves $c = 0.27$ (left) and $c = 0.12$ (right). Bottom: amplitudes of branches of solitary waves shown with circles on free surface and with crosses on the interface. The value of c_{-min}=0.29 is shown with dotted line

An interesting extension of this work would be to include heavy elastic plates and investigate if solitary waves can exist in this setting. Very recently, Akers *et al* [14] have computed travelling periodic waves when a heavy elastic plate is separating two fluids.

Funding. This research has been partially supported by the EPSRC under grant EP/J019305/1.

References

1. Korobkin A, Părău EI, Vanden-Broeck J.-M. 2011. The mathematical challenges and modelling of the hydroelasticity. *Phil. Trans. Royal Soc. A.* **369**, 2803-2812.
2. Squire VA. 2011. Past, present and impendent hydroelastic challenges in the polar and subpolar seas *Phil. Trans. R. Soc. A* **369**, 2813-2831.
3. Părău E and Dias F 2002. Nonlinear effects in the response of a floating ice plate to a moving load. *J. Fluid Mech.* **460**, 281-305.
4. Guyenne P and Părău EI 2012. Computations of fully-nonlinear hydroelastic solitary waves on deep water. *J. Fluid Mech.* **713**, 307-329
5. Guyenne P and Părău EI 2014. Finite depth effects on solitary waves in a floating ice sheet. *J. Fluids Struct.* **40**, 242-262.
6. Milewski PA., Vanden-Broeck J-M and Wang Z. 2011. Hydroelastic solitary waves in deep water. *J. Fluid Mech.* **679**, 628-640.
7. Gao T and Vanden-Broeck J-M. 2014. Numerical studies of two-dimensional hydroelastic periodic and generalised solitary waves. *Phys. Fluids* **26**, 087101.
8. Gao T, Wang Z and Vanden-Broeck J-M. 2016. New hydroelastic solitary waves in deep water and their dynamics. *J. Fluid Mech.* **788**, 469-491.
9. Guyenne P and Părău EI 2017. Numerical study of solitary wave attenuation in a fragmented ice sheet. *Phys. Rev. Fluids* **2**, 034002.
10. Kim G and Davis D 1995. Hydrodynamic instabilities in at-plate-type fuel assemblies. *Nuclear Engineering and Design* **158**, 1-17.

11. Huang L 1995. Flutter of cantilevered plates in axial flow. *J. Fluids Struct.* **9**, 127-147.
12. Ambrose DM and Siegel M 2017. Well-posedness of two-dimensional hydroelastic waves. *Proc. Roy. Soc. Edinburgh A: Math.* **147** (3), 529-570.
13. Liu S and Ambrose DM 2017. Well-posedness of two-dimensional hydroelastic waves with mass. *J. Diff. Eq.* **262** (9). 4656-4699.
14. Akers BF, Ambrose DM and Sulon DW. 2017 Periodic traveling interfacial hydroelastic waves with or without mass. *arXiv preprint*:1704.02387.
15. Blyth MG, Părău EI and Vanden-Broeck J-M 2011. Hydroelastic waves on fluid sheets. *J. Fluid Mech.* **689**, 541-51.
16. Deacon NP, Părău EI, Purvis R and Whittaker RJ 2015. Nonlinear flexural waves in fluid?filled elastic channels. *J. Fluids Struct.* **52**, 16-36.
17. Moni JN and King AC 1995. Guided and unguided interfacial solitary waves. *Q. J. Mech. Appl. Maths.* **48**. 21-38.
18. Părău E and Dias F 2011. Interfacial periodic waves of permanent form with free-surface boundary conditions. *J. Fluid Mech.* **437**, 325-336.
19. Woolfenden HC and Părău EI 2011. Numerical computation of solitary waves in a two-layer fluid. *J. Fluid Mech.* **688** 528-550.
20. Părău EI and Woolfenden HC 2012. Gap solitary waves in two-layer fluids. *IMA J. Appl. Math.* **77**, 399-407.
21. Wang Z, Părău EI, Milewski PA and Vanden-Broeck J-M 2014. Numerical study of interfacial solitary waves propagating under an elastic sheet. *Proc. R. Soc. A* **470**, 20140111.
22. Plotnikov PI and Toland JF 2011. Modelling nonlinear hydroelastic waves. *Phil. Trans. Roy. Soc. A: Math. Phys, Eng. Sci.* **369**, 2942-2956.
23. Laget O and Dias F 1997. Numerical computation of capillary-gravity interfacial solitary waves.*J. Fluid Mech.* **349**, 221-251.
24. Vanden-Broeck JM 1980. Numerical calculation of gravity-capillary interfacial waves of finite amplitude. *Phys. Fluids* **23**, 1723-1726.
25. Wang Z, Vanden-Broeck JM and Milewski PA 2013. Two-dimensional flexural-gravity waves of finite amplitude in deep water. *IMA J. Appl. Math.* **78**, 750-761.
26. Craig W, Guyenne P and Sulem.C 2012. The surface signature of internal waves. *J. Fluid Mech.* **710**, 277-303.